MECHANIKA TEORETYCZNA
I STOSOWANA
Journal of Theoretical
and Applied Mechanics
1, 32, 1994

SHORT FATIGUE CRACK GROWTH IN LASER HARDENED MEDIUM CARBON STEEL

DOROTA NATKANIEC

Department of Mechanical Engineering and Robotics
Technical University of Mining and Metallurgy, Cracow

STANISŁAW KOCAŃDA

Department of Mechanical Engineering
Military Technical Academy, Warsaw

KEITH JOHN MILLER

Department of Mechanical and Process Engineering
University of Sheffield, UK

Short fatigue crack behaviour in laser hardened medium carbon steel (0.45% C) smooth specimens subjected to reversed torsion ($R = -1$) was investigated. The plots of crack length distribution, crack growth and crack growth respectively rate versus number of cycles were presented. Characteristic features of a mechanism of cracking in specimens with various laser track geometry were established on the basis of observations made through SEM and TEM.

1. Introduction

Short fatigue cracks have been intensely analysed since 1975 so they were observed more earlier not being named as short cracks. This item is not defined perfectly and therefore several definitions are applied to determine these cracks. One of these is that short cracks initiate and grow at a high stress level. The other is that their length is compared with grains size i.e. microstucturally short cracks. In the case of physically short cracks their length corresponds with a plastic zone size at the crack tip. Short crack growth rate decreases to a threshold value and then increases as long cracks which are determined by one of the expressions $dl/dN = f(l),(N),(K)$ in terms of linear elastic fracture mechanics (LEFM). Stress intensity factor K_{th} can be set any distinguish item to differ the short and long crack ranges. Short crack growth period is sometimes treated on as an initiation period for cracking. Many works show an important role of microstructural factors in influencing on short crack growth and their anomalous behaviour which can not be analysed by the LEFM principles because of large scale plasticity effect at the crack tip. The short crack regime has been performed on the Kitagawa-Takahashi diagram (cf Kocańda S. and Kocańda A., 1989) which was firstly presented during the 2nd Int.Conf. on "Mechanical behaviour of metals" in Boston, (1976). The principles and basic expressions concerning short crack growth problem established by numerous authors in 1979 $\div$ 1985 have been inserted into the publication mentioned above. The edition of Miller and Rios (1986) encloses 34 works widely analysing the influence of construction, technological, material, geometrical factors and corrosion environment on short crack growth development together with the possibility of crack growth description by fracture mechanics equations. Special issue of the journal Fatigue and Fracture of Engineering Materials and Structures (1991) is devoted to the short cracks problem and contains the papers presented during the conference organized by Miller in Sheffield (UK) in December 1990. Continuously increasing number of edited publications can not be presented hereby but prove the weigth of considern problem.

The results of investigations of short crack behaviour in laser hardened 0.45% C steel specimens are presented here. The subject of this work is extensive study which include the research into short crack growth in specimens with non-treated surface layer, with laser treated or shot-peened surface. The study of fatigue crack behaviour in laser hardened steel specimens, their structure, microhardness and residual stress distribution was reported by Kocańda and Natkaniec (1991a,b), (1992b,c) and presented during the conference in 1991 in Borków (Kocańda and Natkaniec (1992a).

2. Experiments and results

Hour-glass shape specimens of normalized 0.45% C steel were heat treated by an 1.5 kW power continuous wave CO_2 laser in air and at room temperature.

A nitrogen-oxygen atmosphere was provided at the specimens surface. The laser beam velocity was equal to 20 mm/s. The laser tracks of a 3 $\div$ 4 mm

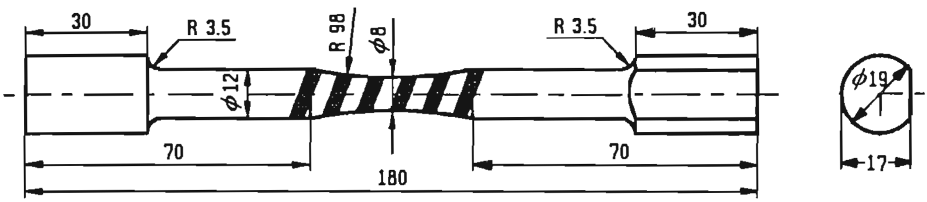

Fig. 1.

width were carried out on the gauge specimen surface in two different manners: circumferentially with a stroke of a 3.5 mm (Fig.1) or covering the surface by overlapping laser tracks. Laser track cross-section of semi-eliptical shape proved a hardened steel structure until the depth of a 0.7 mm. The hardened zone contained a fine grained martensite in the surface layer and martensitic-bainitic mixture at the bottom of laser track. An average microhardness of surface layer was a 600 HV_{100} and sharply droped to a 200 HV_{100} in a pearlitic-ferritic structure of the matrix material. Prior to fatigue tests the sample surface was polished by a diamond paste to 1 μm and then ligthly etched in 0.5% nital and 4% picric acid to reveal microstructural barriers for crack advance.

Fatigue tests were conducted under load control reversed torsion at 5 Hz of frequency in the SIRIUS laboratory in University of Sheffield. Surface shear stress amplitude was calculated on the basis of Nadai's relationship relative to an applied torque for elasto-plastic range. Short fatigue crack growth was monitored by taking plastic replicas from the specimen surface at given intervals of load cycles N_i. By using the Vickers hardness penetrator the marks of piramides were made on sample surface to select the same places on all replicas for crack growth examination. Length of each selected crack was measured with the aid of an optical microscope equiped with an image analysis system. Further microobservations were made through a scanning (SEM) and transmission (TEM) electron microscopes. For the TEM observations were prepared separate replicas shadowed by platinum or chromium to reveal characteristic features of short cracks.

The examination of fracture surfaces aided to establish a mechanism of cracking in the samples with different geometry of laser tracks.

In specimens with circumferential laser tracks the short cracks were found to initiate mainly in slip bands formed in enlongated ferrite grains preferentially orientated to maximum shear stresses or rarely in triple points of grains in non-hardened zone, between the laser tracks only. Short cracks grew in di-

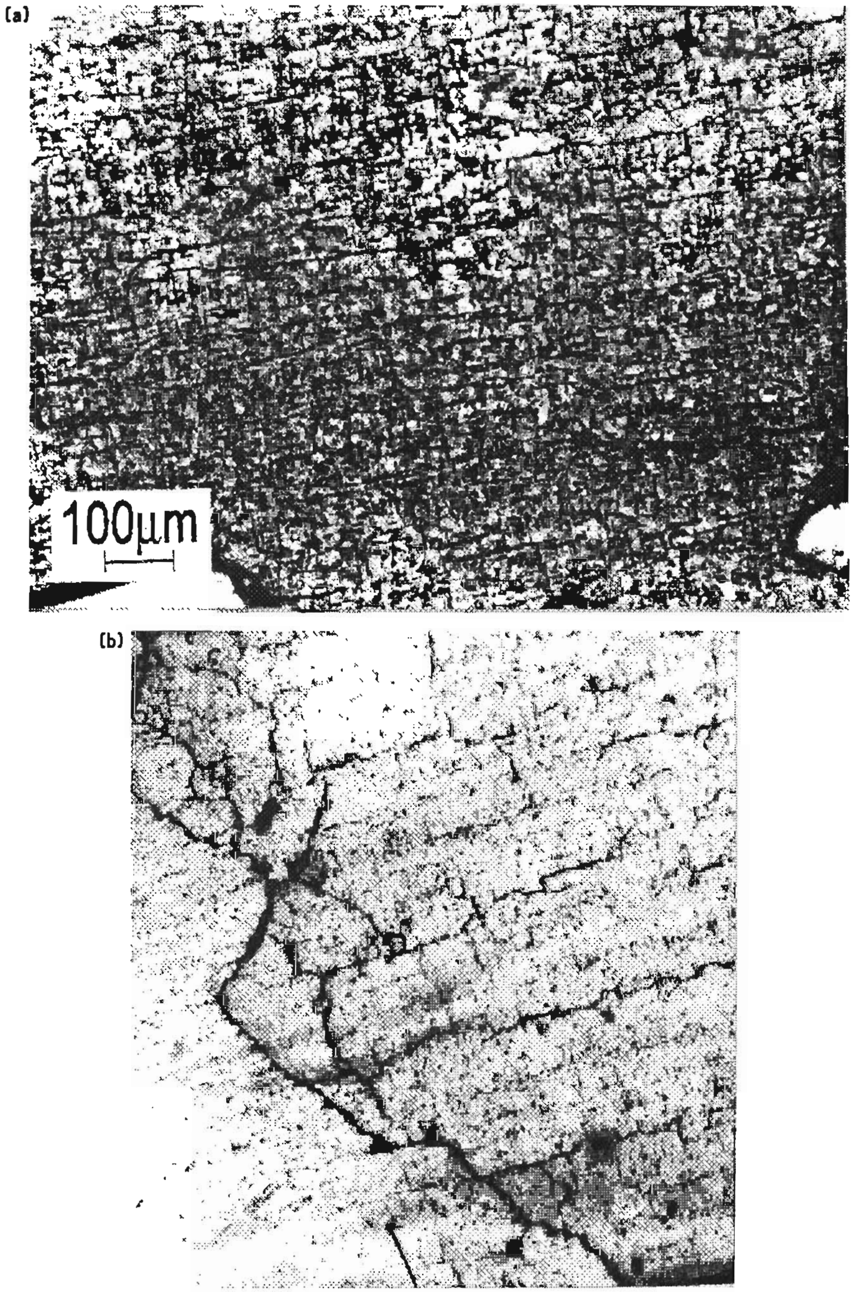

Fig. 2.

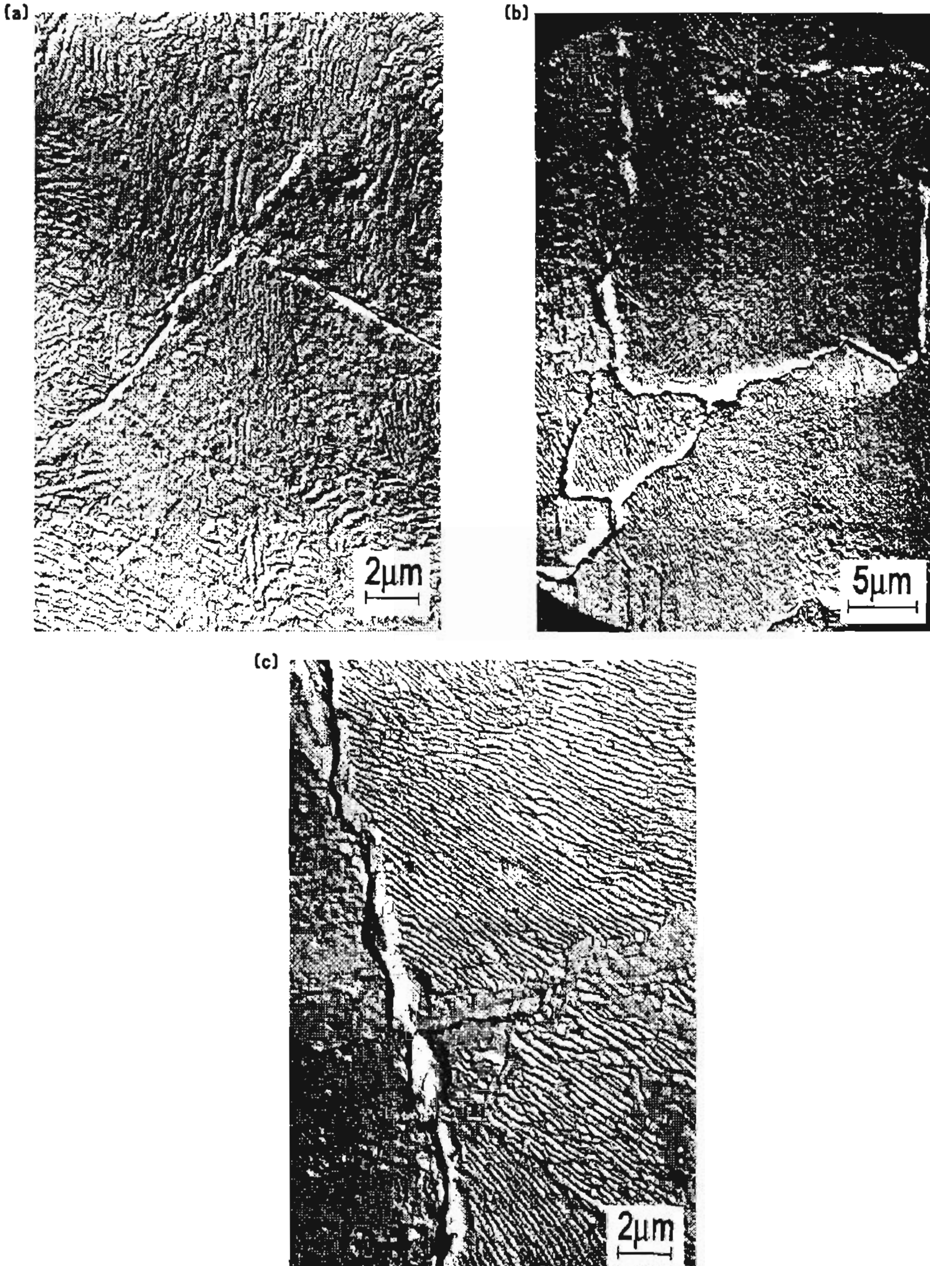

Fig. 3.

rections parallel and perpendicular to the sample axis creating a net of cracks on the specimen surface (Fig.2a,b). Dominant cracks grew in direction according to the sample axis because of structural bands formed in rolling process and orientated along that axis. Short cracks growth was microstructurally dependend. The cracks were deccelerated or temporary arrested at subgrains or grains boundaries and at pearlite colonies (Fig.3a,b). In a transition zone – in the vicinity of laser tracks (Fig.2b) the cracks branched at nearly 45° angles to sample axis and advanced on in direction of maximum normal stresses. In Fig.2b (magn. 50×) the laser track is placed on the left side of the image. Cracks were completely arrested at the border between the laser track and the matrix and finally grew along that border (Fig.3c). The structure of laser track and compressive residual stresses acted there constituted a strong barrier for the cracks.

Another image of crack behaviour were observed in the specimens with overlapping laser tracks. Individual cracks initiated in local melted spots and advanced in direction of maximum normal stresses. The cracks formed mutually crossing systems on the sample surface.

Surface short cracks analysis revealed great number of microcracks in an unit area i.e. 150 ÷ 200 cracks/mm^2. This exceptionally great number of microcracks initiated during fatigue life and mentioned by other authors too can set such a characteristic feature of short cracks. On the other hand, great density of microcracks formed in early stage of fatigue process proves a necessity to improve the prediction of fatigue life of machine parts. Distribution of surface cracks length in the sample with circumferential laser tracks (τ_{app} = 196 MPa) against cycle ratio N_i/N_f (N_f – number of cycles to failure) shows the column diagram (Fig.4a). Cracks less than 10 μm were disregarded in this analysis. There may be found any regularity in cracks advance with an increase of cycle ratio. The rise of crack density is seen for cracks of 50 ÷ 100 μm of length in the range of a $0 \div 0.24 N_i/N_f$ fraction of cycles to failure. A decreasing tendency of shortest crack density is set at the value of $N_i/N_f = 0.54$. In further stage of fatigue process ($N_i/N_f > 0.54$) the variation of microcracks density is connected with new created cracks and crack joining alternatively. Simultanuously, the number of longer cracks increases regularly during the fatigue process. Microcracks initiation activity begins since 1 ÷ 3% of cycles to failure for the specimens with circumferential laser tracks signed as NL1, NL2, L4, respectively, depending on applied stress level and it approaches then a saturation stage (Fig.4b). Greater crack population can be found at lower stress level and the saturation stage is achieved earlier than at higher stress. The plot marked as gl4 relates to non-treated sample.

Short crack growth rate behaves characteristically in the I stage of fatigue

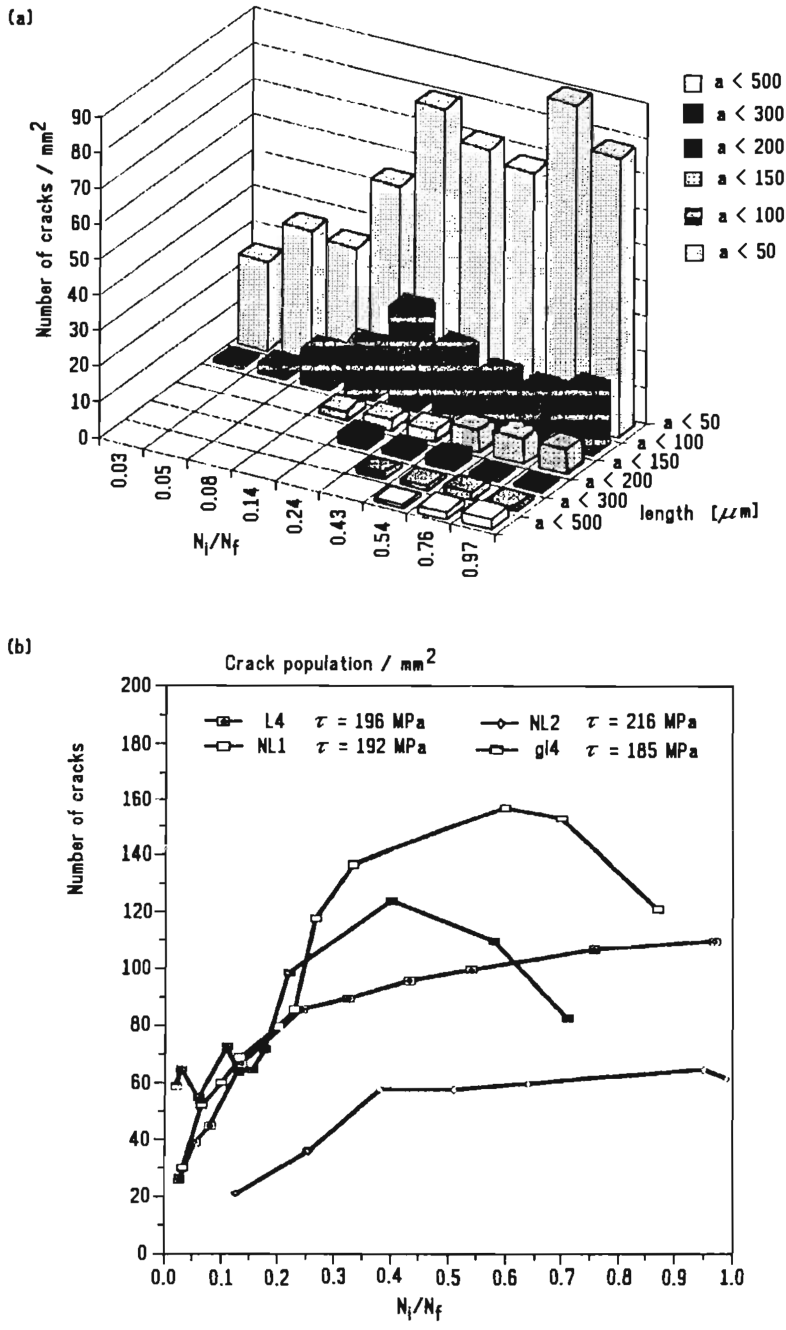
(a)
Number of cracks / mm2
90
80
70
60
50
40
30
20
10
0
0.03
0.05
0.08
0.14
0.24
0.43
0.54
0.76
0.97
Ni/Nf
a < 500
a < 300
a < 200
a < 150
a < 100
a < 50
length [μm]
(b)
Crack population / mm2
Number of cracks
L4 τ = 196 MPa
NL1 τ = 192 MPa
NL2 τ = 216 MPa
gl4 τ = 185 MPa
200
180
160
140
120
100
80
60
40
20
0
0.0
0.1
0.2
0.3
0.4
0.5
0.6
0.7
0.8
0.9
1.0
Ni/Nf

Fig. 4.

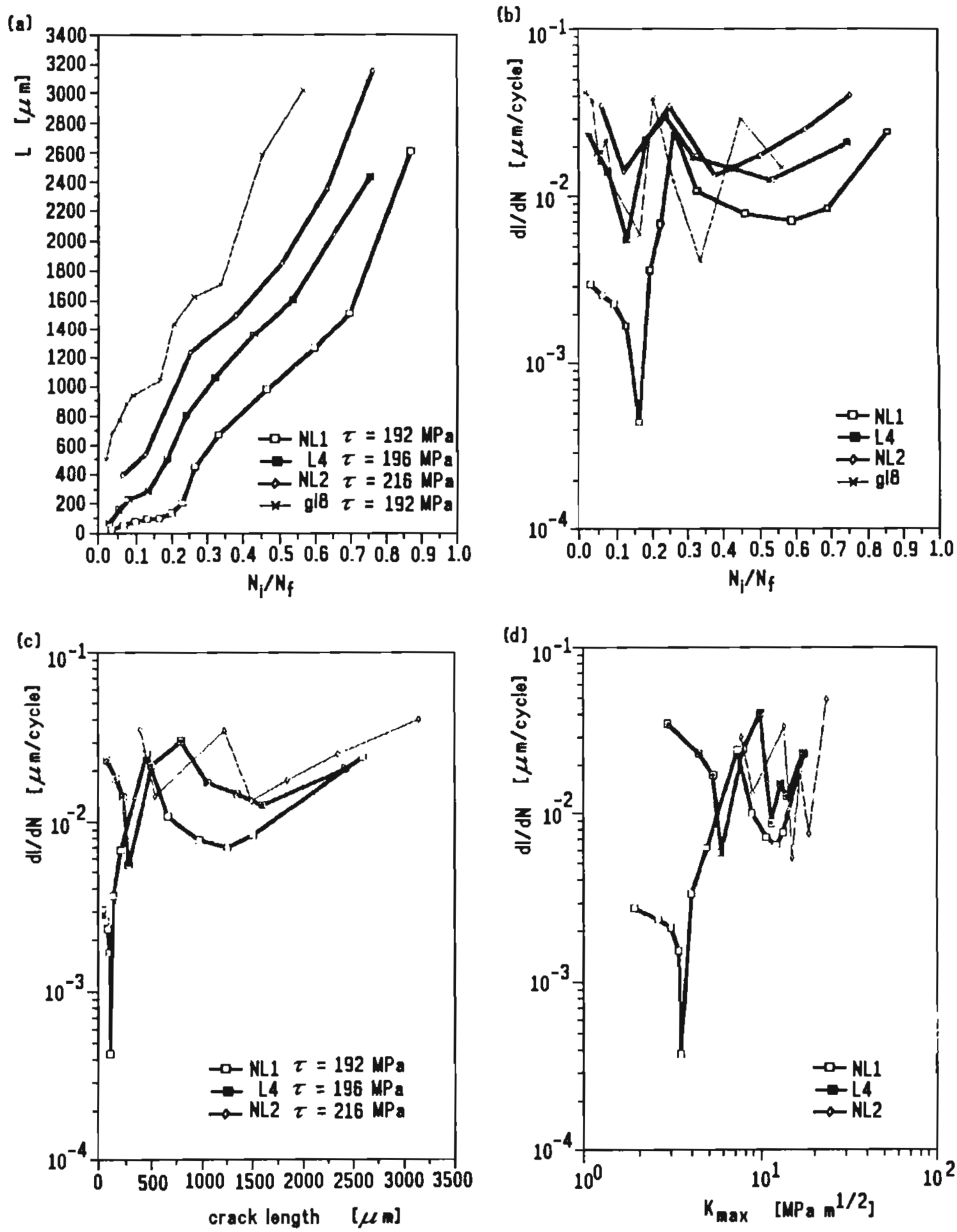
(a)
L [μm]
N_i/N_f
NL1 τ = 192 MPa
L4 τ = 196 MPa
NL2 τ = 216 MPa
gl8 τ = 192 MPa
(b)
dl/dN [μm/cycle]
N_i/N_f
NL1
L4
NL2
gl8
(c)
dl/dN [μm/cycle]
crack length [μm]
NL1 τ = 192 MPa
L4 τ = 196 MPa
NL2 τ = 216 MPa
(d)
dl/dN [μm/cycle]
K_{max} [MPa m^1/2]
NL1
L4
NL2

Fig. 5.

process. In the samples with circumferential laser tracks the crack growth rate dl/dN successively decreases with an increase of crack length until $200 \div 300$ μm (Fig.5). The courses of surface crack growth and crack growth rate versus N_i/N_f or crack length show Fig.5a,b and Fig.5c, respectively. The drop of growth rate relates to a decceleration or temporary arrest of the crack extention at the microstructural barriers. Then crack growth rate sharply increases until the stage when the cracks achieve a next structural barrier. It is interesting that for the specimens tested at various shear stress levels the change of slope of the crack growth rate plots occurs at slightly differet values of N_i/N_f. In the II stage of fatigue the short crack growth rate alters irregularly. The plots of crack rate recall a saw course with variable amplitude. The plot of dl/dN versus $K_{\max}$ – maximum stress intensity factor for the II crack mode shows Fig.5d. The curves of dl/dN indicate dependence of material microstructure in a wide range of the sample fatigue life. For a comparison the plots of crack growth and crack growth rate in non-treated sample gl8 were performed in Fig.5a,b also.

Short crack growth rate dependence on microstructural parameters in the case of specimens with circumferential laser tracks can be expressed by relations given below. For microcracks initiated in a slip band and advance inside a grain the equation given by Rios et al. (1984) is in a form

$$\frac{dl}{dN} = w\frac{\beta\tau - \tau_0}{G}\frac{D - l}{D} \tag{2.1}$$

where

- D – average length of slip bands
- l – length of crack
- G – shear modulus
- τ – applied shear stress
- τ_0 – internal friction stress opposing a movement of dislocations
- β – orientation factor
- w – weigth factor (for e.g. a fraction of dislocations on the slip bands which take part in the process of crack extention).

Crack growth rate of short cracks extended inside a ferrite band of length d_i was determined on the basis of experimental data in form of

$$\frac{dl}{dN} = C(d_i - l)^{\alpha} \qquad \alpha = 0.3 \div 0.35 \tag{2.2}$$

where d_i – length of ferrite band limited by pearlite colony.

In further stage of cracking the course of dl/dN can be fitted by expression

$$\frac{dl}{dN} = Cl^{\alpha}(d-l)^{\beta} \qquad \alpha = 0.4 \qquad \beta = \frac{\alpha}{2} \tag{2.3}$$

where d – average distance between the structural barriers.

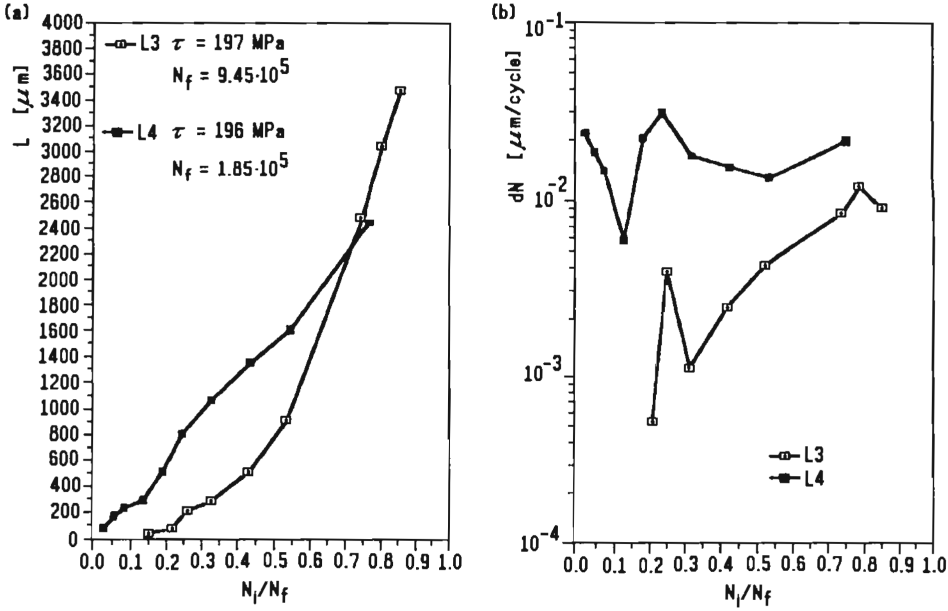

Fig. 6.

In specimens with another geometry of laser tracks – with overlapping surface tracks we do not observe microstructural dependence of short crack growth rate because of a homogeneously hardened structure of the matrix material. For the comparison there were performed in Fig.6a,b the dl/dN plots for the sample ($L4$) with circumferential laser tracks and one with overlapping tracks ($L3$). A dominant crack initiated significantly later in the $L3$ sample than in the other one tested at the same stress level. The crack growth rate was really lower during whole fatigue term and the fatigue life several times longer in the case of the $L3$ sample despite of a higher brittlness of hardened structure of matrix material. For cracks extended in hardened matrix their growth rate can be determined by relation

$$\frac{dl}{dN} = C\Big(\frac{N_i}{N_f}\Big)^{\alpha} \qquad \alpha = 1.8 \div 2.0 \tag{2.4}$$

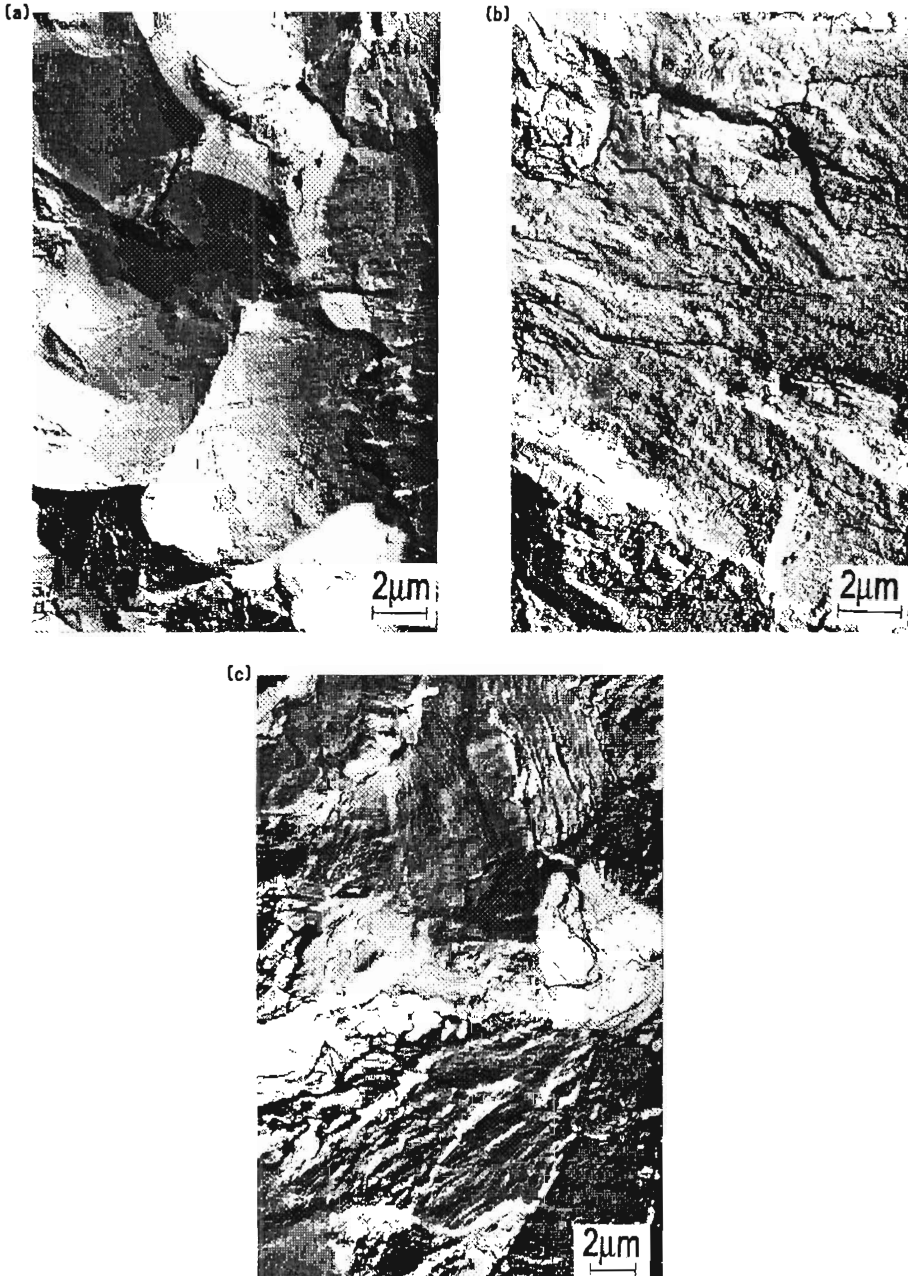

Fig. 7.

The differences of fatigue behaviour in the samples with different geometry of laser tracks can be explained through a favourable surface residual stress state only but not linked to the properties of hardened structure of the matrix. The measurements of surface residual stresses provided compressive stresses in the middle of laser tracks of values $600 \div 700$ MPa and tensile stresses of 200 MPa between the laser tracks in the $L4$ sample. Exclusively compressive stresses ought to be expected in the case of whole hardened gauge surface in the $L3$ sample.

Microobservations of fracture surfaces revealed the spots of crack initiation and provided more details of mechanism of cracking. Examination of fracture surfaces proved a cleavage or quasi-cleavage fracture mainly in the surface layer of laser track in specimens with circumferential laser tracks (Fig.7a). In general, brittle fracture – along grain boundaries and a mixed brittle fracture – partly transgranular and partly as cleavage fracture appeared very rarely in the surface layer. In martensitic-bainitic structure was found quasi-cleavage fracture with certain sympthoms of plastic deformation (Fig.7b). There was observed plastic fracture with fatigue striations in the matrix (upper part of the micrograph Fig.7c) and quasi-cleavage fracture in the laser track (lower part of the micrograph) in transition zone between the matrix and the laser track. In the specimens with overlapping laser tracks there was found generally brittle fracture – along grain boundaries and cleavage planes in the melted area. Final stage of specimens fracture developed in laser tracks.

3. Summary

Short cracks were initiated in slip bands formed in ferrite grains mainly or in triple points of grains in non-hardened zone of the matrix material in laser hardened medium carbon steel specimens. The microcracks advanced in directions of maximum shear stresses in the I stage of cracking process. On sample surface the cracks created a net of mutually perpendicular microcracks. The cracks were deccelerated or temporary arrested at the microstructural barriers. Cracks were completely arrested at the border of laser tracks and the matrix material. Characteristic features of surface microcracks are: high crack density in an unit area and significant drop in crack growth rate in the I stage of fatigue process. In the specimens with overlapping laser tracks we did not observe characteristic behaviour of microcracks. These specimens characterize long fatigue life and lower crack growth rate comparative to the specimens with

circumferential laser tracks. It can be linked to high compressive residual stresses acted in homogeneously hardened surface layer.

Microobservations of fracture surfaces made through SEM and TEM revealed mechanism of final stage of sample failure.

References

1. KOCAŃDA S., KOCAŃDA A., 1989, *Low cycle fatigue of metals,* PWN, Warszawa, (in Polish)

2. KOCAŃDA S., NATKANIEC D., 1991a, *Crack initiation and propagation in a laser hardened 45 steel,* (in Polish), Biul. WAT, 6, 23-46

3. KOCAŃDA S., NATKANIEC D., 1991b, *Theoretical model of residual stresses in steel elements caused by laser treatment,* (in Polish), Arch.Mater.Sci., 13, 141-161

4. KOCAŃDA S., NATKANIEC D., 1992a, *Crack growth rate in laser hardened 45 steel specimens,* (in Polish), Letters of Świętokrzyska Polytechnik, Mechanika 48, 141-152

5. KOCAŃDA S., NATKANIEC D., 1992b, *Fatigue crack initiation and propagation in laser hardened medium carbon steel,* Fatigue and Fracture Engng.Materials and Structures, **15**, 2, 1237-1249

6. KOCAŃDA S., NATKANIEC D., 1992c, *Residual stresses and fatigue crack propagation in a laser hardened medium carbon steel,* Int.Conf. on Localized Damage II, Southampton, (UK)

7. MILLER K.J., DE LOS RIOS E., edit., 1986, *The behaviour of short fatigue cracks,* EGF Publications 1, Mech.Engng.Publications, London

8. DE LOS RIOS E., TANG Z., MILLER K.J., 1984, *Short crack fatigue behaviour in a medium carbon steel,* Fatigue and Fracture Engng.Materials and Structures, **7**, 2, 97-108

9. *Int.Conf. on Short Fatigue Cracks, 10-14 December 1990, Sheffield, (UK),* Fatigue and Fracture of Engng.Materials and Structures., Special issue, **14**, 2/3, 1991

Rozwój krótkich pęknięć zmęczeniowych w laserowo hartowanych próbkach ze stali 45

Streszczenie

Zbadano powstawanie i rozwój krótkich pęknięć zmęczeniowych w laserowo hartowanych próbkach ze stali 45 przy symetrycznym skręcaniu. Podano wykresy przyrostu długości pęknięć i prędkości ich rozwoju oraz wykres gęstości pęknięć w zależności od liczby cykli obciążenia. Omówiono charakterystyczne cechy pękania w próbkach o różnej geometrii strefy zahartowanej.

Manuscript received October 1, 1993; accepted for print October 14, 1993